Partial line-tying of the flute mode in a magnetic mirror

Guy Vandegrift and Timothy N. Good
Physics Department, University of California, Irvine, California 92717

(Received 8 February 1984; accepted 29 October 1985)

The amount of electron emission required to partially line-tie the $m = 1$ flute mode is measured on an axisymmetric mirror-confined plasma. The results are consistent with an ideal magnetohydrodynamic (MHD) calculation with a sheath dissipation term added. The minimum electron emission required is approximately the ion saturation current. The sheath impedance is also calculated for the case when the electron emission exceeds the threshold required for the formation of a virtual sheath.

I. EXPERIMENT

The use of a line-tied blanket to stabilize a mirror-confined plasma against the interchange mode has been described previously.[1-3] The term "line-tying" refers to the ability of an electron emitting endplate to suppress the flute mode by draining the perturbed charge. It has been suggested that the problem of excessive heat loss from the core plasma to the electron emitting endplate can be overcome by line-tying only on an annular blanket that surrounds the hot core plasma. High-order interchange modes that are localized to within the core plasma are stabilized by finite Larmor radius effects.

One problem associated with the application of blanket stabilization to a fusion reactor is the high electron emission required to line-tie plasma. In the blanket stabilization experiments reported earlier,[3] the Richardson thermionic emission from the endplate was comparable to $n_x e v_e$, where $v_e^2 = (2T/m_e)$. In this article, we report that the flute mode is suppressed with an endplate thermionic emission of approximately $n_x e v_i$. (We shall denote T_x and n_x to be the temperature and density near the endplate.) It is convenient to refer to this as "partial line-tying" since the flute mode is not eliminated, but merely reduced in amplitude.

The experiment was performed on the Irvine Mirror Experiment[4] (see Fig. 1). The mirror is axisymmetric with a variable mirror ratio. The wall diameter is 29 cm and the distance between mirror throats is 115 cm. A typical midplane magnetic field is 1 kG. Typical base pressure is 2×10^{-6} Torr. The plasma was heated by 5 kW of input rf power at the ion-cyclotron resonance frequency (ICRF). The plasma was produced by contact ionization of potassium on a thermionically emitting rhenium hot plate.[5] The density at the midplane of the mirror was 10^{10} cm^{-3}. The strong degree of line-tying from the source hot plate was more than adequate to stabilize the ICRF heated plasma against the flute mode. Therefore, a double grid was placed in front of the source near the mirror throat. When both grids were biased to approximately the plasma potential, they had a 60% transparency. In order to de-line-tie the plasma from the source, the grids were pulsed with approximately 5 V for the grid facing the source, and approximately -5 V for the grid facing the plasma. The ICRF was shut off simultaneously with the pulsing of the grids.

The partial line-tying was achieved by heating a lanthanum-hexaboride (LaB_6) plate, located outside the throat opposite to the grids. This plate was biased to the floating potential. The boundary between the de-line-tied core and the blanket is defined by a 1.2 cm radius stainless steel disk placed in front of the LaB_6 plate. This disk maps ($r^2B = \text{const}$) to a radius of 2 cm at the Langmuir probes, where the plasma radius was measured to be 3 cm. The four Langmuir probes were placed near the midplane and were equally spaced azimuthally. The probes were biased to collect the ion saturation current.

The LaB_6 electron emission was measured by placing a probe 1 mm from the plate. The probe I–V characteristic was generated in the absence of plasma, and the saturated "temperature limited" current was recorded. At high emission levels, corresponding to the last three data points in Fig. 2, the probe characteristics did not saturate. The values indicated are the unsaturated current collected at a probe bias of 90 V. The electron emission from the LaB_6 could be varied by varying the power that heated the LaB_6 endplate.

The flute mode instability of the experiment was initiated by the grid pulse that cut off the plasma from its source. During the plasma decay the instability caused a radial displacement of the full length of the plasma column. Moving as a rigid body, this radial displacement was accompanied by an $\mathbf{E}\times\mathbf{B}$ rotation about the magnetic axis. The source electric field for this rotation was the steady state radial field associated with an "electron-rich"plasma produced by con-

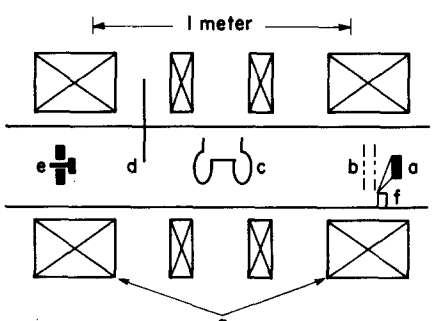

FIG. 1. Schematic experiment showing (a) hot plate plasma source, (b) double grid, (c) ICRF antenna, (d) Langmuir probes, (e) annular electron emitting ring (LaB_6), (f) potassium oven, (g) the coils that create the axisymmetric magnetic field.

 0031-9171/86/020550-06$01.90

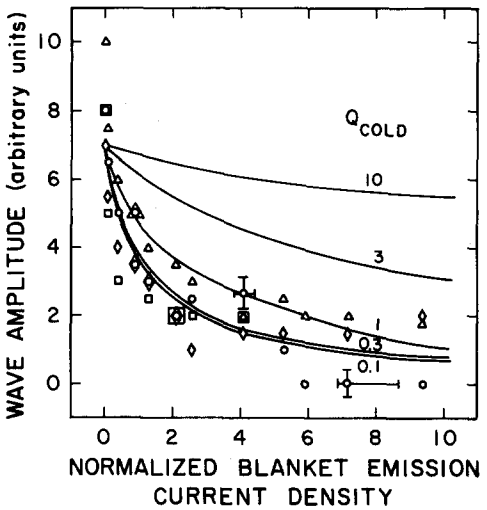

FIG. 2. "Wave amplitude" versus normalized electron emission. The normalized wave amplitude is determined by measuring the heights of each peak shown in Fig. 4, and normalizing the amplitude for each probe to the amplitude of the wave when there is no electron emission. The solid lines show the theoretical reduction in growth rate for different values of $Q(\text{cold}) = \gamma_{\text{MHD}}/2\nu_0$.

tact ionization on a hot plate. Thus the composite motion of the plasma perpendicular to the magnetic field was a spiraling of the plasma column toward the vacuum chamber wall. The plasma motion parallel to the magnetic field consisted of two parts. A streaming component of ions was drifting away from the source hot plate because of sheath acceleration at the hot plate. Some of these ions were heated by the ICRF, thereby moving their pitch angles out of the loss cone. The heated ions were reflected by the magnetic mirror and executed the bouncing motion of a sloshing ion distribution, until they were lost by collision or velocity space diffusion back into the loss cone.

The observed $m = 1$ interchange mode is shown in Fig. 3. The mode appeared as peaks in the density as measured by the stationary probes 1–4, which are located near the peak

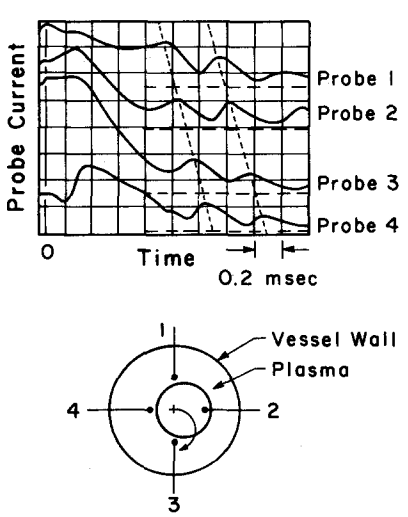

FIG. 3. "Flute" evolution showing $n_i(t)$ at $r = 3$ cm, and $\theta = 0°$, 90°, 180°, and 270°. Time $t = 0$ marks when the double grid isolates the plasma from the hot plate source. The lower picture shows schematically the position of the plasma relative to the four probes during the evolution of the mode.

density gradient. The real part of the wave frequency $\text{Re}(\omega)$ was approximately 6×10^3 sec^{-1} with the wave rotating in the electron diamagnetic direction. The arrow marks the time when the grid de-line-tied the plasma from the source. The initial peak after the grid pulse is not believed to be related to the flute mode. This initial peak after the grid pulse appears to have a $m = 0$ structure, which suggests that it is caused by a longitudinal sound wave excited by the grids. Another possible explanation for this first response of the probes is that the ICRF depressed the plasma edge density, while helping to drive the mode unstable by increasing the ion temperature. Since the ICRF was shut off simultaneously with the grid pulse, the first density peaks may have been a relaxation from the ICRF-heated radial density profile. The wave amplitude was actually decreasing in time because much of the plasma left the chamber during the evolution of the mode. Thus we expect agreement with theory to be at best qualitative.

In order to document the relation between the flute mode and the endplate emission, we have continuously varied the emission in Figs. 4(a) to 4(f). In Fig. 4(a), the LaB_6 plate was heated to the threshold of observable emission in order to keep it clean. We define the amplitude by the largest oscillations that appear on the density decay oscillogram after the initial response to the grid pulse. The lack of symmetry on the four probe signals may be attributed to asymmetric density profiles, different radial probe positions, and different collection areas for the probes.

The points in Fig. 2 correspond to the wave amplitude versus the normalized blanket emission J_R/nev_B, where J_R is the thermionic blanket emission, $n = 10^{10}$ cm^{-3}, and $v_B = 2.2\times10^5$ cm/sec is the average parallel velocity of the plasma to the endplate. (This value of v_B corresponds to 1 eV of ion drift energy and was measured by pulsing the plasma source off with the grids and measuring the time required for the plasma to exit the machine axially.)

II. THEORY

In order to model this wave, we employ a linearized zero-beta fluid equation. The mode amplitude is assumed of the form $\phi(r)\exp(im\theta - i\omega t)$. The unperturbed density varies as $\exp(-r^2/r_0^2)$ and $E_\theta = im\phi/r$ is governed by [6–8]

$$E_\theta'' + \left(\frac{3}{r} - \frac{2r}{r_0}\right)E_\theta' - \left(\frac{m^2-1}{r^2} + \frac{2}{r_0^2}\frac{\omega^2 + m\omega_G^2 + 2i\nu}{\omega(\omega - m\omega_D)}\right)E_\theta = 0, \quad (1)$$

where $\omega_D = 2T_{iL}/eBr_0^2$ is the diamagnetic frequency that represents finite ion Larmor radius effects. The curvature is represented by the classical flute mode growth rate ω_G, and the line-tying parameter ν is related to endplate emission by

$$\nu = \nu_0(1 + J_R/J_B), \quad (2)$$

where J_R is the Richardson electron emission current and $J_B = n_x e v_B$ is the ion current striking the endplate. In Eq. (2) we model the effect of an annular line-tied blanket by allowing ν to depend on r. Equation (2) is valid provided the Richardson electron emission is weak enough so that the unperturbed electrostatic potential rises monotonically from

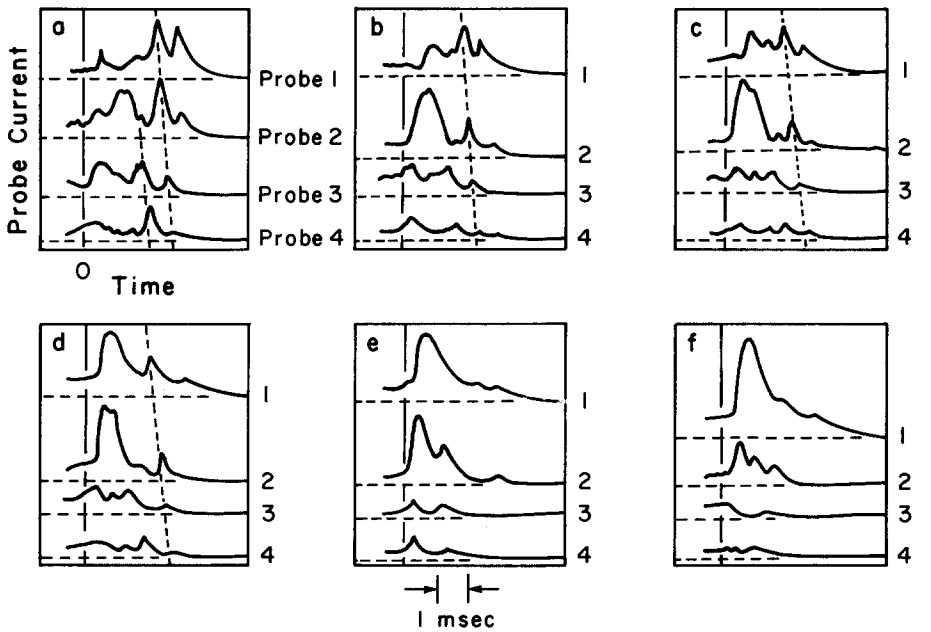

FIG. 4. Mode evolution versus electron emission on the LaB_6 electron emitting ring. Figures (a) through (f) correspond to a normalized electron emission of 0, 0.06, 0.42, 0.96, 1.3, and 2.1, respectively. The electron emission is normalized to the ion saturation current nev_B.

the endplate into the plasma. For $J_R \gtrsim J_B$, it is believed[9,10] that the potential at the sheath is not monotonic. In Sec. III we will consider this possibility.

For Eq. (1), we will employ the ideal magnetohydrodynamic (MHD) equations to obtain ω_G. The connection between Eq. (1) and the more approximate MHD model for the $m = 1$ mode can be seen directly from Eq. (1). If ω_D is greater than ω, ν, and ω_G, then only the last term in Eq. (1) is important. The dispersion relation is given by Eq. (10), and the mode amplitude is nearly uniform, with $|E''_\theta| < |E_\theta/r_0^2|$ and $|E'_\theta| < |E_\theta/r_0|$. In our case, the validity of Eq. (10) was checked numerically using a computer code written by Segal.[11] The tendency of a large ω_D to force $E_\theta(r)$ to be constant for the $m = 1$ mode was also demonstrated in reference [12]. The assumption of a uniform E_θ greatly simplifies the analysis and allows us to transform the ideal MHD model into a circuit model as we now show.

The circuit model is more than an analogy. Using Eqs. (4), (7), and (8) we can relate the perturbed potential to the total perturbed current crossing a plane that intersects the axis of the plasma. To the extent that the mode is flutelike, and that $E_\theta(r)$ is constant, the plasma really is a capacitor, an inductor and a resistor in parallel. (Note that we use cgs units.)

We consider an axisymmetric mirror of length l_p, with a magnetic field $B(z)\hat{z}$ that has the mirror throats ($dB/dz = 0$) at $z = \pm \frac{1}{2} l_p$. For simplicity we consider a plasma with a radius $R(z)$. The density and pressure are arbitrary in the z direction, but are assumed to be uniform for $r < R(z)$ and vanish for $r > R(z)$. By magnetic flux conservation, $R^2(z)B(z)$ is constant along z. Following the ideal MHD equations, we consider a perturbation and construct an energy principle. We denote velocity by $-i\omega$, and assume a z-dependent electric field in the y direction, $E = \phi/2R(z)$. It is more physical to consider the perturbed voltage $\phi(z)$ instead of the usual displacement ξ. The two perturbations are related by the $\mathbf{E}\times\mathbf{B}$ drift formula: $-i\omega\xi = c\phi\hat{x}/2R(z)B(z)$. The kinetic energy associated with this perturbation is

$$T = \tfrac{1}{2} C_\perp \phi^2, \tag{3}$$

where

$$C_\perp = \frac{1}{16}\int dz\, \epsilon(z) \simeq \frac{1}{16}\epsilon l_p, \tag{4}$$

where $\epsilon = 4\pi c^2 M n(z)/B^2(z) = \omega_{pi}^2/\Omega_{ci}^2$.

We have chosen our perturbation so that the only nonvanishing term in the ideal MHD "potential" energy is the contribution resulting from curvature:

$$U = -\int d^3\mathbf{x}(\boldsymbol{\xi}\cdot\nabla P)(\boldsymbol{\xi}\cdot\mathbf{K}), \tag{5}$$

where $\mathbf{K} = d^2R/dz^2\,\hat{r}$ is the magnetic field line curvature.[8,13] This energy integral can be written

$$U = (1/2\omega^2) L_\perp^{-1} \phi^2, \tag{6}$$

where $-\phi^2/\omega^2 = (\int \phi\, dt)^2$, and

$$L_\perp^{-1} = \frac{c^2}{16}\int dz\, \beta(z) R^{-1}(z) R''(z) \simeq \frac{c^2}{8}\frac{l_p}{l_T^2}\beta, \tag{7}$$

$$\beta(z) = 8\pi P(z)/B^2(z).$$

The approximation after Eq. (7) is good for a large mirror ratio and a magnetic field that is uniform in the center and rises to the peak value in a length l_T at each mirror throat.

Next we consider the energy dissipation resulting from line-tying. The perturbed potential is $x\phi/2R(z)$. The current density that flows out of the plasma to the endplate is $Y(x\phi/2R(z))$ where $Y = \delta J/\delta\phi$ is the "sheath conductance." If we assume that the plasma is terminated by identical sheaths at each end, the energy dissipated per unit time is

$$\frac{dU}{dt} = R_s^{-1}\phi^2, \tag{8}$$

where $R_s^{-1} = \pi r_x^2 Y/8$, and r_x is the plasma radius at the endplate. We adopt the Kunkel–Guillory model for the sheath conductance: $Y = v_B n_x e^2/T_x$, where n_x, T_x are the

density and electron temperature of the external plasma, respectively, and v_B is the drift velocity of the ions striking the endplate. The sheath resistance R_s is

$$R_s = \frac{8}{\pi r_x^2} \frac{T_x}{n_s e^2 v_B}. \tag{9}$$

From (3), (6), and (8), we obtain the dispersion relation

$$\omega^2 + \omega_G^2 - 2i\nu\omega = 0, \tag{10}$$

where $\omega_G^2 = 1/L_\perp C_\perp$ and $2\nu_0 = 1/R_s C_\perp$.

Equations (4) and (7) have been integrated using the magnetic field of the Irvine Magnetic Mirror, assuming constant density and pressure for $\frac{1}{2}l_p < z < \frac{1}{2}l_p$. For mirror ratio μ between 2 and 9, the following equations are valid to within 10%:

$$\omega_G = 1.9(1 + \mu/12)(v^*/l_p)\ln\ \mu, \tag{11}$$

$$\nu_0 = 0.4\left(1 + \frac{\mu}{12}\right)^2 \frac{v_B}{l_p} \frac{n_x}{n_0} \frac{r_x^2 M_i \Omega_i^2}{T_x}, \tag{12}$$

where n_x, T_x, and r_x are the external density, electron temperature, and plasma radius, respectively, $\Omega_i = eB/M_i c$ is evaluated at the mirror midplane, $v^* = \sqrt{T^*/2M_i}$ with $T^* = \frac{1}{2}(T^e + T^i)$, and v_B is the drift velocity of plasma striking the endplate.

The parameter $Q = \omega_G/2\nu$ describes the degree to which line-tying influences the mode. By particle conservation, we have $n_x r_x^2 v_B = \alpha n_0 r_0^2 v_i/\mu$, where n_0 and r_0 are referenced to the midplane, v_i is the average drift velocity of the ions exiting the mirror throat, and α is the probability that an ion impinging upon the mirror throat will leave the machine. The Q of a partially line-tied flute mode for a mirror ratio of 5 is thus

$$Q = \frac{Q_c}{1 + J_R/J_B}, \tag{13a}$$

$$Q_c = 4\alpha \frac{a_i^2}{r_0^2} \frac{T_x}{T_i} \frac{v^*}{v_i}. \tag{13b}$$

The physical significance of Q is that line-tying is unimportant if $Q \gg 1$, and that for small Q, the growth rate is reduced to $Q\omega_G$. We see from Eq. (13) that a simple mirror with a radius of 10 Larmor radii must have an axial confinement of 25 bounces before line-tying becomes unimportant. Equation (13a) shows the reduction of Q caused by an emitting endplate.

We can extend this formalism to the case of quadrupole magnetic fields.[14] The extension is accomplished by inserting a factor $e(z)$ into the integrand of Eq. (4) and into the integrand of Eq. (7). In Eq. (7) we redefine the normalized field line radius $R(z) = (e/B)^{1/2}$. Here e is the ratio of plasma diameter in the x direction to plasma diameter in the y direction. This extension to the quadrupole geometry is valid for a perturbed electric field in the y direction.

Another extension of the model is possible if the mirror is line-tied at only one end or if the line-tying occurs only at the outer edge of the plasma. This will increase Q in Eq. (13) by a numerical factor obtained by limiting the area of integration described above Eq. (8). For line-tying at only one end, Q is increased by a factor of 2, and for edge line-tying, the increase in Q depends on the assumed density profile. For a square radial density profile, with uniform density for $r < r_x$, zero density for $r > r_x$, and line-tying only within $r_w < r < r_x$, Q is increased from the value given in Eq. (13a) to the value Q':

$$Q' = \frac{Q}{1 - (r_w/r_x)^4}. \tag{14}$$

For our experiment $r_w/r_x = 0.67$, and only one end is line-tied so that Q increases by a factor of 2.5.

III. SHEATH ADMITTANCE OF A VIRTUAL CATHODE

Equations (2) and (8) describe the influence of line-tying when the unperturbed field line increases monotonically from the endplate to the center of the mirror. Now we consider the possibility that electron emission from the endplate causes a virtual cathode to be formed near the hot plate (see Fig. 5). The physical mechanism responsible for the formation of the virtual cathode is similar to the familiar Bohm sheath criterion that says that the ions must enter the sheath region with a minimum directed energy. If the ions enter the sheath region with insufficient initial velocity, the sheath will have a negative charge as the streaming ions are swept through the sheath. (Since $n_i v_i$ is constant, n_i decreases as v_i increases.) In much the same manner, cold electrons that are emitted from the endplate contribute to a negative charge density in the sheath because these electrons travel more slowly near the endplate. By Poisson's equation a negatively charged sheath causes the second derivative of the potential to be positive. This may cause the potential to roll over, forming the virtual cathode shown in Fig. 5.

We start by calculating the equilibrium potential between the plasma and the virtual cathode, shown as V in Fig. 5. We consider the region to the right of the virtual cathode; three species of particles are present. The plasma ions are assumed to enter from the right with a monoenergetic spectrum with energy $E = 1/2M_i v_i^2$. The primary electrons enter from the right with a half-Maxwellian of temperature T. The secondary electrons come from the left with temperature $\theta T < T$. Our calculation follows that of Refs. 10 and 11, except that we do not demand that the net current to the endplate vanish. If we calculate the z-dependent charge density of each species, Poisson's equation can be written

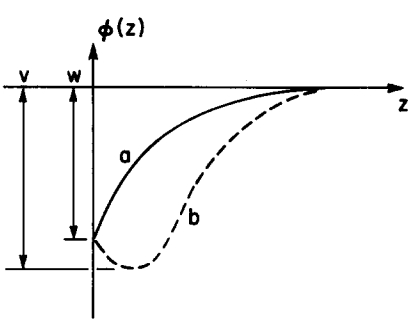

FIG. 5. Schematic drawing of the potential near the endplate, without a virtual endplate, without a virtual cathode (a), and with a virtual cathode (b).

$$\frac{d^2\eta}{ds^2} = aX[(V-\eta)^{1/2}] + bX\left[-\left(\frac{V-\eta}{\theta}\right)^{1/2}\right] - \left(\frac{E}{E+\eta}\right)^{1/2}, \tag{15}$$

where

$$\eta = -e\phi/T_e, \quad s = z/\lambda_e, \quad \lambda_e^2 = T_e/4\pi ne^2, \tag{16}$$

$$X(x) = e^{x^2}\int_{-\infty}^{x} dt\, e^{-t^2},$$

and the plasma ion energy E and the virtual cathode to plasma potential V are normalized to kT_e. The constants a and b are normalized densities of the primary and secondary electrons, respectively. We demand that the plasma be neutral far from the sheath (i.e., $\eta'' \to 0$ as $s \to \infty$). This yields

$$1 - aX(\sqrt{V}) - bX(-\sqrt{V/\theta}) = 0. \tag{17}$$

We define δ to be the normalized net current density leaving the plasma: $\Sigma J = \delta\sqrt{T}/2m_e$, where

$$\delta = \tfrac{1}{2}a - \tfrac{1}{2}b\sqrt{\theta} - E(m_e/M_i)^{1/2}. \tag{18}$$

Following Ref. 11, we reduce Eqs. (15)–(17) to a more convenient form by multiplying by $2(d\eta/ds)$ and integrating by parts. Taking the limits of integration to be at $s = \infty$ and at the virtual cathode yields

$$\begin{aligned} &I_e + I_R + I_i = 0, \\ &I_e = -2a[X(\sqrt{V}) - \sqrt{\pi}/2 - \sqrt{V}], \\ &I_R = -2b\theta[X(-\sqrt{V/\theta}) - \sqrt{\pi}/2 + \sqrt{V/\theta}], \\ &I_i = 4[(E^2 + EV)^{1/2} - E]. \end{aligned} \tag{19}$$

[We note that this result was published in Ref. 10, but Eq. (13) of Ref. 10 appears to be a misprint. The author of Ref. 10 may have obtained the correct equation in his own notes because Figs. 3 and 4 of Ref. 10 are obtained from this equation and appear to be correct.]

Equations (17)–(19) are three equations in four variables: δ, a, b, and V. We are interested in the solution near the "floating potential" of the virtual cathode: $\delta = 0$. Using the approximations for the error function of Ref. 15, one can numerically obtain the functions $\delta(V)$ and $b(V)$. The sheath admittance is related to $\partial\delta/\partial V$ near $\delta = 0$. However, we do not wish to vary the plasma-to-virtual cathode potential V, but the plasma-to-wall potential W (as shown in Fig. 5). If the emission from the wall is kept constant during the fluctuations in δ, V, and W, we have the constraint

$$b\exp[(V-W)/\theta] = \text{const}. \tag{20}$$

Strictly speaking, Eq. (20) applies only when the emission is thermionic, since fluctuations in potential are accompanied by density fluctuations that would produce fluctuations in the secondary emission current. However, this produces a small correction to the sheath admittance when $\theta \ll 1$. An elementary application of calculus to Eq. (20) yields

$$\frac{d\delta}{dW} = \frac{d\delta}{dV}\left(1 + \frac{\theta}{b}\frac{db}{dV}\right), \tag{21}$$

and the sheath admittance follows from $Y = (T/2m_e)^{1/2}\, d\delta/dW$.

For practical fusion applications, the temperature of the emitted electrons θT is much less than the primary electron temperature T. From the equations, one can show that both Y and J_R/J_B should tend to a constant value for $\theta \ll 1$. This was verified for $\theta = 0.1$, 0.02, and 0.005.

We have calculated the ratio of emitted electron current, J_R/J_B, and the sheath admittance Y/Y_{KG} for two cases. (Here $Y_{KG} = v_B ne^2/T_e$ is the Kunkel–Guillory result for a nonemitting cathode.)

Figure 6 shows the case for a hot reactor plasma with deuterium (a.m.u. = 2) and $\theta = 0.02$. In this case J_R/J_B is in the range of 1 to 6 (depending on the incident ion energy), and the virtual sheath is formed at moderate values of electron emission. The case appropriate for the parameters of the Irvine Mirror is shown in Fig. 7, and it can be seen that a virtual sheath is formed at values of J_R far higher than were used in the experiment.

One should keep in mind the limits to the validity of this model of the sheath admittance. The Kunkel–Guillory article[7] includes other terms that are usually small. Prater[16] considers a contribution to j_i caused by density fluctuations instead of potential fluctuations. This effect can be important if a net unperturbed current is flowing axially to the endplate on a given field line. (Otherwise, the electron and ion contributions to this effect cancel.) Also, both this calculation and the aforementioned calculations assume that the mean free path for electrons is smaller than the machine length. This assumption was implicitly made when we assumed a half-Maxwellian for the electron distribution function.

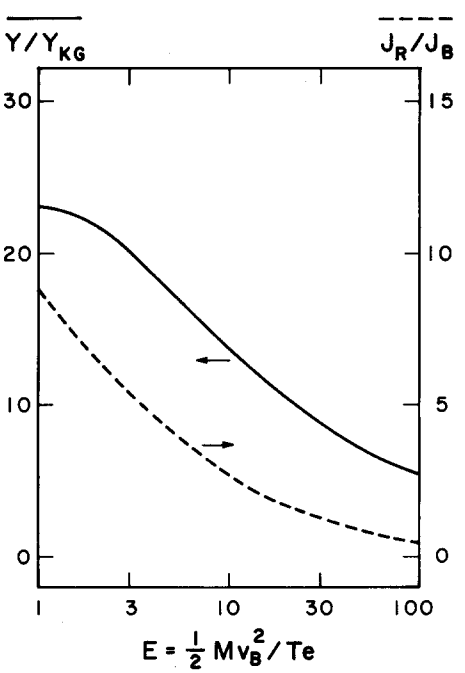

FIG. 6. Solid line: normalized sheath admittance y, as a function of incident ion energy ($y_{KG} = nev_B/T_e$). Dotted line: ratio of electron current emitted from the endplate to ion saturation current, nev_B. Both curves represent a hot deuterium plasma with a cold emitted electron temperature $T_R = \theta T_e$ with 0.02.

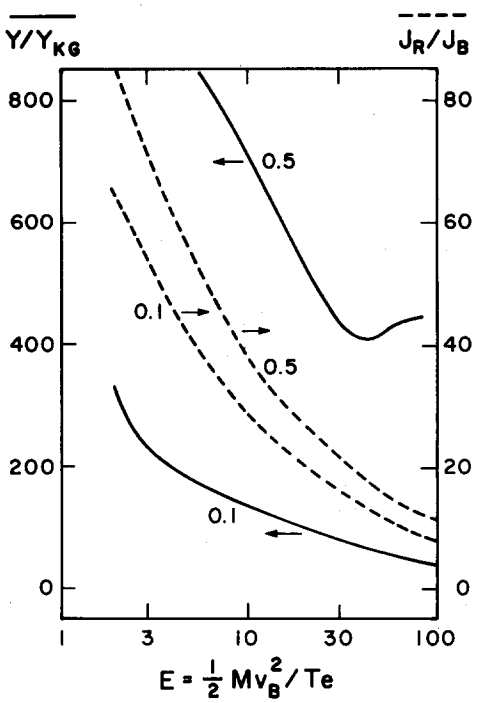

FIG. 7. Solid lines: normalized sheath admittance as a function of incident ion energy. Dotted line: ratio of emitted electron current to ion saturated current. Both curves represent a barium plasma (a.m.u. = 137), with two values of the emitted electron temperature $T_R = \theta T_e$: $\theta = 0.5$ and $\theta = 0.1$.

IV. CONCLUSION

We have shown that: (1) partial line-tying is important for any mirror that does not confine the particles for enough bounces [α^{-1} in Eq. (12)]; (2) in order to increase line-tying in such a plasma, it is only necessary to have a Richardson's emission of a few times the ion saturation current.

The solid lines in Fig. 2 show the theoretical reduction in growth rate based on Eq. (10) assuming different values of Q for the nonemitting endplate. The curves of Fig. 2 assume that the sheath is monotonic, so that Eq. (13) describes the change in Q as the plate is heated. The amplitude is normalized to 7 for each value of Q (cold). As we heat the endplate to electron emission, Q is reduced by the factor shown in Eq. (2) or Eq. (13), and the amplitude is reduced. The wave amplitude seems to match the theoretical growth rate if we take Q (cold) < 1. This is intuitively reasonable: increasing the degree of line-tying will not drastically change the mode unless line-tying is already an important effect. One should not misconstrue the fit between theory and experiment in Fig. 2, since it is comparing amplitude with growth rate. Note that the wave frequency is comparable with the inverse of the plasma lifetime.

We have also obtained the sheath admittance for an endplate when the electrons are emitted from the plate copiously enough so that a virtual cathode forms in front of the plate. This admittance is independent of the degree of emission (provided it exceeds the critical value for virtual cathode formation); but it does depend on the ratio of incident ion energy to primary electron temperature. This sheath admittance can be used to include partial line-tying in the dispersion relation for either curvature-driven or radial-electric field-driven flute modes, and for ideal MHD ballooning modes.

The calculation also suggests a method for measuring the effect of line-tying already present in present mirror fusion experiments where MHD stability limits have been found, and where it is possible to change the electron emission in a controllable manner.

We conclude by suggesting what would happen to the flute mode in a mirror-confined plasma if the endplate electron emission were continuously increased from zero to a few times the ion saturation current (leaving all other plasma parameters unchanged). The result would depend on whether the confinement was good enough for $Q_c \ll 1$ in Eq. (13). For a well-confined plasma, we would not expect much change in the flute mode. However, if $Q_c \lesssim 3$, we expect the growth rate to decrease as the endplate emission increases.

ACKNOWLEDGMENTS

The authors would like to acknowledge useful discussions with Dr. Nathan Rynn, Dr. Roger McWilliams, Dr. G. D. Porter, and the assistance of Robert Noel, Mason Okubo, Fred Kinley, and Virgil Laul.

This work was supported by the U.S. Department of Energy, Office of Energy Research under Contract No. PA-DE-AT03-76ER53026.

[1] B. Lehnert, Phys. Fluids **9**, 1367 (1966).
[2] R. F. Post, R. E. Ellis, F. C. Ford, and M. N. Rosenbluth, Phys. Rev. Lett. **11**, 166 (1960).
[3] D. Segal, M. Wickham, and N. Rynn, Phys. Fluids **25**, 1485 (1982).
[4] G. Vandegrift, T. N. Good, and N. Rynn, Bull. Am. Phys. Soc. **28**, 1048 (1983).
[5] N. Rynn, E. Hinnov, and L. C. Johnson, Rev. Sci. Instrum. **38**, 1378 (1967).
[6] M. Wickham and G. Vandegrift, Phys. Fluids **25**, 52 (1982).
[7] M. Rosenbluth, N. A. Krall, and N. Rostoker, Nucl. Fusion Suppl. Part I, 143 (1962).
[8] W. K. Kunkel and J. Guillory, *Proceedings of the 7th International Conference on Phenomena in Ionized Gases,* Belgrade, 1965, edited by B. Perovic and D. Tosic, (Gradjevinska Knjiga Publishing House, Belgrade, 1966), Vol. 2, p. 702.
[9] G. D. Hobbs and J. A. Wesson, Plasma Phys. **9**, 85 (1967).
[10] G. D. Porter, Nucl. Fusion **22**, 1279 (1982).
[11] D. Segal, Phys. Fluids **26**, 2565 (1983).
[12] M. W. Phillips and J. D. Callen, Phys. Fluids **27**, 1733 (1984).
[13] M. A. Lieberman and S. L. Wong, Plasma Phys. **19**, 745 (1977).
[14] G. Vandegrift, Ph.D. thesis, University of California, Berkeley, 1982.
[15] M. Abramowitz and I. Stegun, *Mathematical Tables* (Dover, New York, 1970).
[16] R. Prater, Phys. Fluids **17**, 193 (1974).